Hindawi Publishing Corporation
Journal of Nanomaterials
Volume 2011, Article ID 876287, 6 pages
doi:10.1155/2011/876287

Research Article

Ti/Al Ohmic Contacts to n-Type GaN Nanowires

Gangfeng Ye, Kelvin Shi, Robert Burke, Joan M. Redwing, and Suzanne E. Mohney

Department of Materials Science and Engineering, The Pennsylvania State University, University Park, PA 16802, USA

Correspondence should be addressed to Suzanne E. Mohney, mohney@ems.psu.edu

Received 10 July 2011; Accepted 23 September 2011

Academic Editor: Somchai Thongtem

Titanium/aluminum ohmic contacts to tapered n-type GaN nanowires with triangular cross-sections were studied. To extract the specific contact resistance, the commonly used transmission line model was adapted to the particular nanowire geometry. The most Al-rich composition of the contact provided a low specific contact resistance (mid $10^{-8}\,\Omega\text{cm}^2$) upon annealing at 600 °C for 15 s, but it exhibited poor thermal stability due to oxidation of excess elemental Al remaining after annealing, as revealed by transmission electron microscopy. On the other hand, less Al-rich contacts required higher annealing temperatures (850 or 900 °C) to reach a minimum specific contact resistance but exhibited better thermal stability. A spread in the specific contact resistance from contact to contact was tentatively attributed to the different facets that were contacted on the GaN nanowires with a triangular cross-section.

1. Introduction

The wide bandgap semiconductor GaN has attracted great attention for its use in electronic and optoelectronic devices, and its growth and properties have recently been explored in the form of a semiconductor nanowire (NW) because of its potential for transistors [1] and light emitting devices [2–4]. Most devices fabricated from GaN NWs require low-resistivity and reliable electrical contacts.

Researchers have reported the formation of both Schottky and ohmic contacts to GaN NWs. Sometimes a contact such as Ti/Al [5] has been observed to form either Schottky or ohmic contacts as a result of nonuniformities in the NW surface. The metallizations Ti/Al/Pt/Au [6], Ti/Au [7, 8], Ni/Au [9], as well as Pt deposited by a focused ion beam [10, 11], have all been successfully used to form Ohmic type contacts to n-type GaN nanowires, sometimes with the assistance of annealing or premetallization ultraviolet (UV) ozone surface treatments. On the other hand, Ti, Cr, and Au have been used to form Schottky diodes [7, 12]. These reports also demonstrate that the condition of the NW surface [5, 6] and the size of the GaN nanowire [10] can affect the characteristics of the contact.

In this study, we examine Ti/Al contacts to n-type GaN nanowires by electrically probing the contacts and by examining them in cross-section using transmission electron microscopy (TEM). The contact resistance and specific contact resistance were extracted taking into account the geometry of these nanowires, which are tapered and have triangular cross-sections. The effect of changing the ratio of Ti : Al on the specific contact resistance was also studied as a function of annealing conditions, and differences in the thermal stability of the contacts were correlated to changes in the contact metallurgy.

2. Experimental Procedures

2.1. Contact Preparation. Gallium nitride nanowires (NWs) were fabricated using nickel-catalyzed metalorganic chemical vapor deposition [13]. The NWs have a cross-section that is an equilateral triangle, with the side of a triangle varying from 120 to 300 nm for most of the NWs. An electric field alignment procedure [14] was adopted to place the NWs in desired locations on highly doped Si wafers ($2 \times 10^{19}\,\text{cm}^{-3}$) covered with 100 nm thick SiN_x layers. First, using photolithography, sacrificial Ag electrodes were defined on the SiN_x/Si. The gap between the electrodes ranged from 5 to 20 μm. Next, a photoresist trench was defined with a width slightly larger than the gap between the electrodes. Hence, the electrode gap and a small portion of both electrodes were exposed. Gallium nitride NWs released by sonication

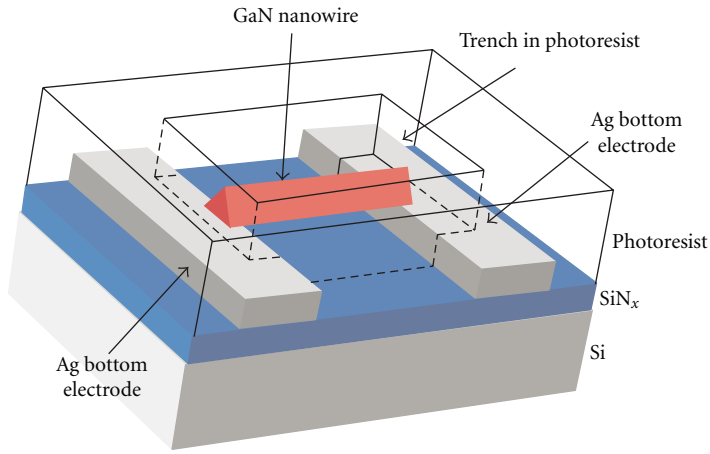

Figure 1: Schematic diagram showing a GaN nanowire aligned within a photoresist trench on Ag electrodes.

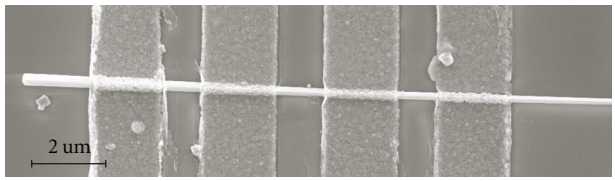

Figure 2: Scanning electron microscopy image of a GaN NW with four contacts.

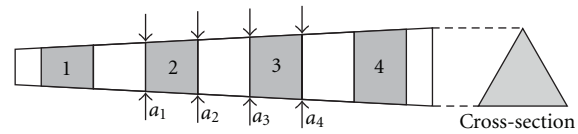

Figure 3: Schematic test structure with exaggerated NW taper and labeling of dimensions and contacts.

into isopropyl alcohol (IPA) were then dropped onto the wafer, a 5–10 V AC voltage (5 kHz) was applied to the Ag electrodes, and nanowires were attracted to the electrodes by dielectropheresis. The sample at this stage of fabrication is shown in Figure 1. Photolithography was again used to prepare four openings in the photoresist for lift-off of four colinear contacts, a descum procedure was performed in an O_2 plasma, and the sacrificial Ag electrodes were etched away using a commercial gold etchant (Transene GE-8148). Then, the GaN NW surface was cleaned using buffered oxide etch (10%), rinsed in deionized H_2O, dried in N_2 gas, and promptly loaded into a vacuum chamber for electron beam evaporation with a base pressure of 2×10^{-7} Torr for Ti/Al deposition. Two different sets of metal layer thicknesses were selected: Ti (36 nm)/Al(80 nm) and Ti(21 nm)/Al(90 nm). These thicknesses correspond to a Ti : Al atomic ratio of 1 : 2.4 (~71 at.% Al) and 1 : 4.6 (~82 at.%), respectively, based on the density of the bulk materials. Using scanning electron microscopy (SEM), a top view of the completed device is shown in Figure 2.

2.2. Measurement and Calculation of Specific Contact Resistance. The calculation of specific contact resistance, ρ_c, required special consideration due to the tapering of the nanowires and their equilateral triangular cross-sections. Four contacts were used along the length of the nanowire, as shown in Figure 3. To measure the resistance of a single contact, we sourced current between pairs of contacts and measured the potential difference between others, as described in this example for the measurement of the resistance of contact 2. First, current was sourced between contacts 1 and 4, I_{14}, and the difference in potential was measured between probes 2 and 3, V_{23}. This measurement provided the resistance of the nanowire between contacts 2 and 3, independent of the resistance of contacts 2 and 3. Next, the current was sourced between contacts 2 and 4, I_{24}, and the potential difference was again measured between contacts 2 and 3, providing V'_{23}. These measurements provided the sum of the resistance of contact 2 and the nanowire segment between contacts 2 and 3. Therefore, the resistance of contact 2, $R_{c,2}$, was calculated using the following equation:

$$R_{c,2} = \frac{V'_{23}}{I_{24}} - \frac{V_{23}}{I_{14}}. \quad (1)$$

The prior four-point probe measurement made by applying I_{14} and measuring V_{23} was also used to calculate the resistivity of the nanowire, assuming a uniform resistivity throughout the nanowire:

$$\rho_s = \frac{\sqrt{3}a_2a_3}{4L_{23}} \frac{V_{23}}{I_{14}}. \quad (2)$$

Field emission scanning electron microscopy was later used to measure the distance between contacts 2 and 3, L_{23}, and the local lengths of the sides of the triangular cross-sections, a_2 and a_3, as shown in Figure 3.

With the resistivity of the nanowire and the resistance of a contact measured, the next step was to determine ρ_c, which for lateral contacts requires the determination of the transfer length, L_T. Adapting the transmission line model for

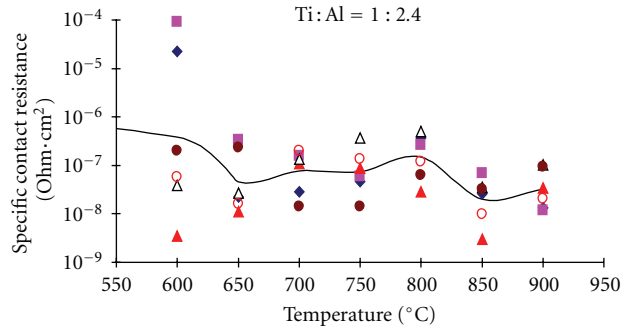

Figure 4: Specific contact resistance versus annealing temperature for the contacts with Ti : Al = 1 : 2.4. The dots in the figures are from different NWs, while the solid line stands for the logarithmic average for all the contacts annealed at the same temperature.

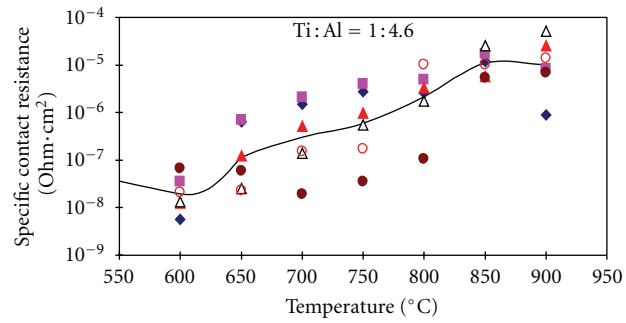

Figure 5: Specific contact resistance versus annealing temperature for contacts with Ti : Al = 1 : 4.6. The dots in the figures are from different samples, while the solid line is the logarithmic average for all the contacts annealed at the same temperature.

a cylindrical nanowire [15] to the case of a triangular cross-section with contacts on two sides of the triangle and using the average length of a side of tapered contact (the average of $a_1 + a_2$ for contact 2), we arrive at the following solutions:

$$L_T = \sqrt{\frac{\sqrt{3}(a_1 + a_2)\rho_c}{16\rho_s}},$$
$$R_{c,2} = \frac{\rho_c}{L_T(a_1 + a_2)} \coth\left(\frac{L}{L_T}\right). \quad (3)$$

Although simplifications can be made for contacts sufficiently longer or shorter than L_T, the transfer length in our samples was sufficiently close to the length of the contact, L, that it was necessary to solve the simultaneous equations numerically to arrive at values of the two unknowns, L_T and ρ_c.

Back gating of the test structures was also performed, verifying the n-type conductivity of the nanowires.

2.3. Materials Characterization. A JEOL 2010F field emission transmission electron microscope (TEM)/scanning TEM (STEM) operating at 200 keV with electron energy loss spectroscopy (EELS) and energy dispersive spectroscopy (EDS) was used to study both the NWs and metallization layer. A FEI Quanta 200 dual-beam focused ion beam (FIB) was used to prepare cross-sectional TEM samples of selected contacts. During the sample preparation, Pt was introduced to form a protective layer above the area of interest. Device dimensions were measured using field emission scanning electron microscopy (FESEM) in a LEO 1530.

3. Results and Discussion

Some of the as-deposited Ti/Al contacts exhibited rectifying behavior, but nearly all contacts became ohmic after annealing. The specific contact resistance is reported after cumulative 15 s rapid thermal anneals in N_2 gas beginning with the lowest annealing temperature of 600°C. For the samples with Ti/Al ratios of 1 : 2.4, the specific contact resistance stabilized near $1 \times 10^{-7}\,\Omega\text{cm}^2$ after annealing at 650°C, as shown in Figure 4, and dipped a bit further after annealing at 850°C. For the more Al-rich samples (Ti/Al ratio of 1 : 4.6), the specific contact resistance reached its minimum in the low $10^{-8}\,\Omega\text{cm}^2$ range after it was annealed at only 600°C for 15 s, and it increased steadily to $\sim 1 \times 10^{-5}\,\Omega\text{cm}^2$ after annealing at 900°C for 15 s, as shown in Figure 5. The nanowire resistivities were generally not affected by annealing, with an average value of 0.013 Ωcm and a standard deviation of 0.004 Ωcm. One outlier had a higher resistivity of 0.037 Ωcm.

A range of specific contact resistance values was measured for each contact composition, with both Figures 4 and 5 showing data points for individual nanowires. There was no correlation between the specific contact resistance and the nanowire resistivity; nanowires with lower resistivities did not necessarily provide lower specific contact resistances, as might be expected due to heavier doping. In addition, no correlation with the size of the nanowire could be made to explain the variation in specific contact resistance.

Figure 6, obtained by cross-sectional TEM, shows that the NW cross-section was in the shape of an equilateral triangular. Diffraction patterns (not shown here) indicate that GaN NWs grew along a <110> direction. Two of the three sides of the nanowire cross-section were {011} planes, and the third was an {001} plane. During contact fabrication, we had no control over which type of facet sat on the surface of the wafer, leaving the other two exposed to contact formation. The variation in contact resistance among different nanowires may in part be due to contacting different crystallographic faces of GaN. In fact, Mastro et al. [16] recently demonstrated that polarization fields in III-nitride nanowires, which vary based on the crystallographic orientation of a facet, can be used to control current transport.

The specific contact resistance as a function of annealing time was also measured. For the sample with a Ti/Al ratio of 1 : 2.4, an annealing temperature of 700°C was selected for repeated anneals, with the cumulative annealing time shown on Figure 7. The specific contact resistance stabilized in less than 1 min. For the 1 : 4.6 samples, a 600°C annealing temperature was selected to age the samples. In this case, the

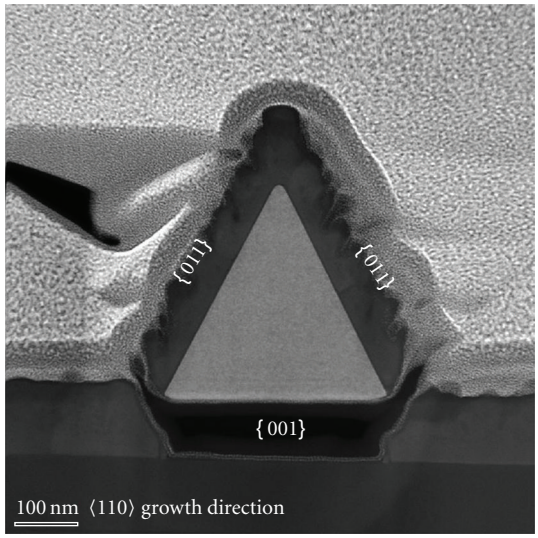

Figure 6: GaN NW cross-section (STEM high angle annular dark field image). The dark regions on the top two sides of the triangle are the contact metallization, while the bright regions are electron beam and Ga ion beam deposited Pt used to protect the sample during preparation of the cross-section in the FIB.

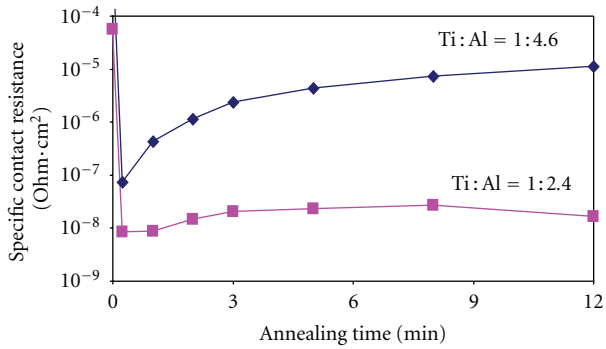

Figure 7: Specific contact resistance versus annealing time at 700°C for a typical contact of each composition.

specific contact resistance increased with longer annealing time, as shown in Figure 7, which displays a typical contact for each composition.

The samples annealed for extended times were examined in detail by transmission electron microscopy. The 1 : 2.4 samples annealed for 12 min at 700°C exhibit a very low specific contact resistance. A thin layer of Ti_2Al [17] immediately adjacent to the GaN is shown in Figure 8, as tentatively identified from the interplanar spacings ($d_{(020)}$ = 0.250 nm and $d_{(002)}$ = 0.232 nm) and angles between these planes from high-resolution TEM. The phase identification was furthermore consistent with the approximate atomic ratio of 2 : 1 for the Ti : Al, as measured by EDS and shown in the line scan in Figure 9. The metallization farther from the interface with GaN was richer in Al than Ti (approximately 3 : 2). Analysis of the GaN/Ti_2Al interface was also performed using EELS (not shown), and no evidence of O or N in the

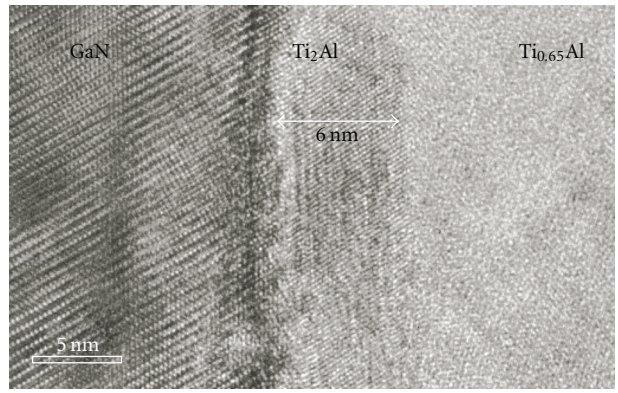

Figure 8: High resolution TEM image of the 1 : 2.4 Ti : Al contact after 12 min at 700°C.

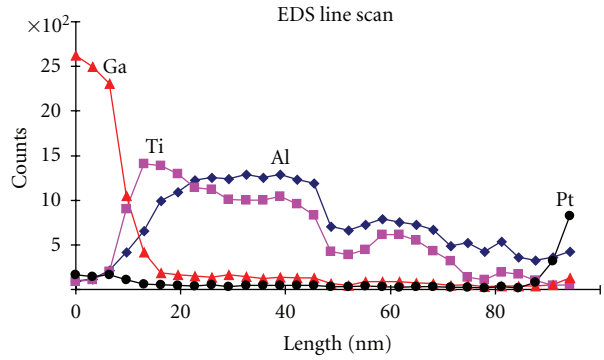

Figure 9: EDS line scan starting within the GaN and traversing the metallization for the 1 : 2.4 contact after 12 min at 700°C. Note that O and N are not plotted due to the low sensitivity of the EDS detector to light elements.

Ti_2Al layer adjacent to the GaN was found. Therefore, the common explanation for ohmic contact formation, which is N vacancies that act as donors are generated in the GaN when nitride reaction products form, is not directly supported by this observation. It is possible that the titanium aluminide has a sufficiently low work function that the barrier height of the contact is adequately lowered to allow ohmic contact formation.

After the contacts were annealed for 12 min at 600°C, the specific contact resistance increased. These degraded contacts were cross-sectioned and examined by TEM. An EDS line scan of the Al-rich 1 : 4.6 contact is shown in Figure 10 following 12 min of annealing at 600°C. Note that O and N are not shown in this plot because of the low sensitivity of the EDS detector to light elements. The composition of the contact metallization appears to be largely homogeneous, although some enrichment of Al is observed at both the contact surface and adjacent to the GaN. While a Ti-Al phase is still observed near the interface with GaN, immediately adjacent to the GaN is an Al-rich layer. No signal for N or Ti was detected by EELS in this location. Rather, a strong O signal was detected here (but no other regions in the sample).

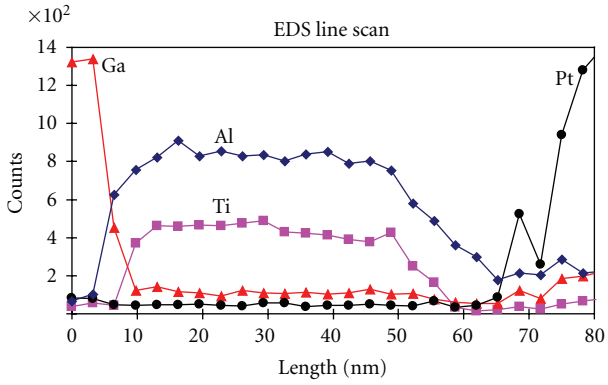

Figure 10: EDS line scan starting in the GaN and crossing the metallization for the 1 : 4.6 contact after annealing for 12 min at 600°C. Note that O and N are not plotted due to the low sensitivity of the EDS detector to light elements.

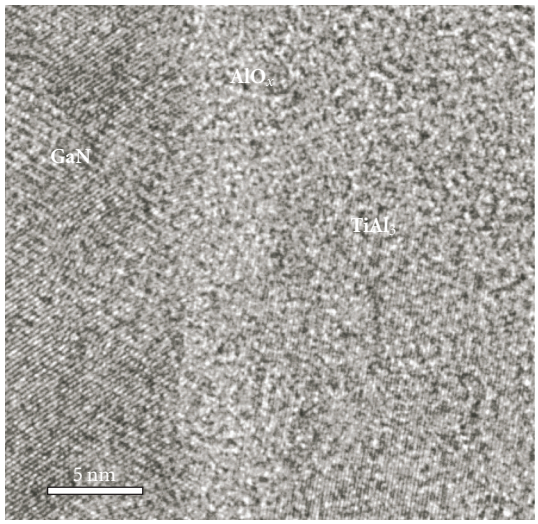

Figure 11: High resolution TEM image of the interface of the Ti : Al contact after 12 min at 600°C. An amorphous layer has been observed next to the GaN NW and contains Al and O based on a combination of EDS and EELS data.

Figure 11 shows an image of this interface obtained by HRTEM. Immediately adjacent to the GaN, where Al is present according to Figure 9 and O was detected by EELS, is an amorphous region labeled AlO_x. The location of this oxide layer explains the increase in contact resistance observed in the aged contacts with the Ti : Al atomic ratio of 1 : 4.6. Next to the oxide layer is a Ti-Al layer with perpendicular interplanar spacings of 0.37 nm and 0.23 nm consistent with $TiAl_3$ [18]. Since $TiAl_3$ is the most Al-rich intermetallic phase on the Al-Ti phase diagram [19], we would expect aluminum remaining after Ti and Al completely react to form $TiAl_3$. Oxidation of this excess Al, which is a liquid at the high annealing temperatures, explains the poorer thermal stability of the contacts with this composition.

4. Conclusions

Ti/Al contacts to n-type GaN nanowires were studied. A change in the Ti : Al ratio in the contacts was correlated with a marked difference in the specific contact resistance as a function of annealing temperature. Contacts with a Ti : Al ratio of 1 : 4.6 became ohmic with a low specific contact resistance in the mid $10^{-8}\,\Omega\text{cm}^2$ range after annealing for 15 s at 600°C but exhibited poor long-term stability at this temperature or upon annealing at higher temperatures. The poor thermal stability was attributed to oxidation of elemental Al remaining after annealing in these Al-rich contacts. On the other hand, contacts with a Ti : Al ratio of 1 : 2.4 exhibited better thermal stability but also required annealing at 850 or 900°C for 15 s to minimize the specific contact resistance. A spread in the specific contact resistance from contact to contact was tentatively attributed to the different facets that were contacted on the GaN nanowire with a triangular cross-section.

Acknowledgments

The authors are grateful to ARO Grant W911NF-09-1-0140 for financial support. The use of the Penn State Nanofabrication Facility (NSF NNUN ECCS-0335765) is also acknowledged.

References

[1] J. R. Kim, H. M. So, J. W. Park et al., "Electrical transport properties of individual gallium nitride nanowires synthesized by chemical-vapor-deposition," *Applied Physics Letters*, vol. 80, no. 19, pp. 3548–3550, 2002.

[2] H. J. Choi, J. C. Johnson, R. He et al., "Self-organized GaN quantum wire UV lasers," *Journal of Physical Chemistry B*, vol. 107, no. 34, pp. 8721–8725, 2003.

[3] F. Qian, Y. Li, S. Gradečak, D. Wang, C. J. Barrelet, and C. M. Lieber, "Gallium nitride-based nanowire radial heterostructures for nanophotonics," *Nano Letters*, vol. 4, no. 10, pp. 1975–1979, 2004.

[4] A. Motayed, A. V. Davydov, M. He, S. N. Mohammad, and J. Melngailis, "365 nm operation of n-nanowire/p-gallium nitride homojunction light emitting diodes," *Applied Physics Letters*, vol. 90, no. 18, Article ID 183120, 2007.

[5] G. Koley, L. Lakshmanan, H. Wu, and H. Y. Cha, "Nanoscale surface characterization of GaN nanowires correlated with metal contact characteristics," *Physica Status Solidi (A)*, vol. 204, no. 4, pp. 1123–1129, 2007.

[6] C. Y. Chang, T. W. Lan, G. C. Chi et al., "Effect of ozone cleaning and annealing on Ti/Al/Pt/Au ohmic contacts on GaN nanowires," *Electrochemical and Solid-State Letters*, vol. 9, no. 5, pp. G155–G157, 2006.

[7] C. Hwang, J. H. Hyung, S. Y. Lee et al., "The formation and characterization of electrical contacts (Schottky and Ohmic) on gallium nitride nanowires," *Journal of Physics D*, vol. 41, no. 10, Article ID 105103, 2008.

[8] M. H. Ham, J. H. Choi, W. Hwang, C. Park, W. Y. Lee, and J. M. Myoung, "Contact characteristics in GaN nanowire devices," *Nanotechnology*, vol. 17, no. 9, pp. 2203–2206, 2006.

[9] E. Stern, G. Cheng, M. P. Young, and M. A. Reed, "Specific contact resistivity of nanowire devices," *Applied Physics Letters*, vol. 88, no. 5, Article ID 053106, pp. 1–3, 2006.

[10] C. Y. Nam, J. Y. Kim, and J. E. Fischer, "Focused-ion-beam platinum nanopatterning for GaN nanowires: ohmic contacts and patterned growth," *Applied Physics Letters*, vol. 86, no. 19, Article ID 193112, pp. 1–3, 2005.

[11] A. Motayed, A. V. Davydov, M. D. Vaudin, I. Levin, J. Melngailis, and S. N. Mohammad, "Fabrication of GaN-based nanoscale device structures utilizing focused ion beam induced Pt deposition," *Journal of Applied Physics*, vol. 100, no. 2, Article ID 024306, 2006.

[12] S. Y. Lee and S. K. Lee, "Current transport mechanism in a metal-GaN nanowire Schottky diode," *Nanotechnology*, vol. 18, no. 49, Article ID 495701, 2007.

[13] R. A. Burke, D. R. Lamborn, X. Weng, and J. M. Redwing, "Growth and process modeling studies of nickel-catalyzed metalorganic chemical vapor deposition of GaN nanowires," *Journal of Crystal Growth*, vol. 311, no. 13, pp. 3409–3416, 2009.

[14] P. A. Smith, C. D. Nordquist, T. N. Jackson et al., "Electric-field assisted assembly and alignment of metallic nanowires," *Applied Physics Letters*, vol. 77, no. 9, pp. 1399–1401, 2000.

[15] S. E. Mohney, Y. Wang, M. A. Cabassi et al., "Measuring the specific contact resistance of contacts to semiconductor nanowires," *Solid-State Electronics*, vol. 49, no. 2, pp. 227–232, 2005.

[16] M. A. Mastro, B. Simpkins, G. T. Wang et al., "Polarization fields in III-nitride nanowire devices," *Nanotechnology*, vol. 21, no. 14, Article ID 145205, 2010.

[17] E. Ence and R. Margolin, "Compounds in the titanium-rich region of the Ti-Al system," *AIME Transactions*, vol. 209, p. 484, 1957.

[18] R. Norby and A. N. Christensen, "Preparation and structure of Al_3Ti," *Acta Chemica Scandinavica, Series A*, vol. 40, p. 157, 1986.

[19] H. Okamoto, "Al-Ti (aluminum-titanium)," *Journal of Phase Equilibria*, vol. 14, no. 1, pp. 120–121, 1993.